Computation of discretization error bounds on the fatigue damage of a shear plate

L. Mell & V. Rey & F. Schoefs
Research Institute in Civil and Mechanical Engineering (GeM)
University of Nantes, France
B. Rocher
Chantiers de l'Atlantique
Saint Nazaire, France

ABSTRACT: Offshore Wind Energy is one of the most promising offshore renewable energies. Bottom fixed offshore wind turbines have reduced step by step their Levelized Cost of Energy. It relies both on CAPEX and OPEX reduction by optimizing the design. One of the key issues is a better assessment of the risks and reliability. As a consequence, the accuracy of the reliability assessement relies on the capacity to perform numerical computations giving accurate results for the safety analysis. In that framework, mechanical and hydrodynamical equations are often solved using discretization techniques such as the finite element method. These methods introduce a discretization error which deteriorates the quality of the analysis. However, bounds on the exact solution on a quantity of interest may be computed *a posteriori*.
This paper focuses on the fatigue assessment of a critical part of Offshore SubStations : the connection between the pile and the jacket. An approach is presented to propagate bounds computed on stress to the damage and guide remeshing in order to reduce the discretization error on the damage.

1 INTRODUCTION

Designing offshore structures requires to ensure its mechanical safety. Therefore, the survival of the structure has to be checked against ultimate, fatigue and accidental limit states. This is usually done by defining a mechanical model of the structure. Partial differential equations arising from it are solved by a discretization technique such as the finite element method (FEM) (Ciarlet 1978). FEM is widely used but introduces a discretization error affecting the mechanical response. However it is possible to estimate, *a posteriori*, the discretization error (Ainsworth & Oden 1997).

Offshore structures are subject to varying loads such as wind and waves. Even within elastic limits, fluctuating stress resulting from these loads may initiate micro-cracks and fatigue rupture. Standard fatigue analysis usually neglects the propapation time as in practice it is usually small compared to the crack initiation phase (Det Norske Veritas 2010). To perform fatigue analysis of crack initiation, a hot spot of the structure needs to be identified. This location is usually a structural detail such as a weld toe or a sharp edge where the crack is likely to appear. The aim of the methods presented in (Det Norske Veritas 2010) is to study stress cycles characteristics at this hot spot. Stress time series in relevant sea state are obtained at the location of the detail. To calculate local stress, recommended practices suggest several methods. The first approach is to use a 3D mesh overlaying at best the detail geometry and having sufficient density to account for stress concentration. This strategy being computationally expensive, simplistic approaches exist and consist in computing the stress close to the hot spot using more simple models such as beam theory, shell theory or 2D analysis. Then, the hot spot stress can be computed using detail dependent stress concentration factors or by extrapolating stresses.

Next, stress cycles within the stress time series need to be identified and rainflow counting is usually performed (Matsuishi & Endo 1968). These stress cycles are then used to calculate the maximum number of cycles before failure using Stress to Number of cycles before failure curves (SN curves). These curves, depending on the studied structural detail, are not deterministic and their parameters might be modeled as random variables for which guidelines give the distribution (Det Norske Veritas 2010). Finally, the survival of the structure subject to fatigue might be checked using Palmgren-Miner rule (Palmgren 1959, Miner et al. 1945) and the cumulative distribution function

of the Gaussian distribution. This procedure results in the estimation of a probability of failure to be compared to standard recommendations. Local stresses depend on the finite element discretization which relies on the choice of the mesh. There is a mitigation between computation time and accuracy. This paper aims at dealing rationnaly with this issue.

This paper proposes an approach to compute bounds on the exact value of the local stress which will be propagated on the stress cycles and finally to damage. These bounds can afterwards guide remeshing in order to reduce discretization error and ensure structural safety with an appropriate computational time.

The structure of this paper is the following. First, the mechanical problem and the computation of the finite element solution of stress at the hot spot is explained. Next, the calculation of error bounds on the exact local stress is described. The derivation of stress cycles within a time series is then explained. Next, the calculation of number of cycles before failure and the computation of the damage using a SN curve is highlighted. Finally, the method to derive bounds on damage is illustrated on the example of the shear plate, the connection between the jacket structure and piles fixing it in the soil.

2 DERIVATION OF HOT SPOT STRESS TIME SERIES FOR JACKET OFFSHORE STRUCTURES

2.1 *Generalities about fatigue analysis*

For jacket structures of electrical substations, fatigue loads are mainly due to waves and currents because of the relative small surface exposed to wind. An accurate description of the phenomena relying on a stochastic wave model is usually implemented. According to (Det Norske Veritas 1996), the main parameters of sea states are significant wave height (H_s), peak period (T_p), main wave direction (θ_0), wave spreading function and wave spectrum model (usually chosen as one side Gamma model) . The distribution of these parameters can either be discretized into a scatter diagram or continuous. Using scatter diagrams is simpler and allows to simulate a small number of sea states (combination of (H_s, T_p, θ_0)) to calculate damage.

For nearly all offshore structures, it is too computationnally expensive to simulate the whole service life. The structural response is therefore simulated for a small period (usually taken between 1 and 3h) for each sea state. Then, the time series is extrapolated to account for the whole service lifetime. To model the structural response, computational fluid dynamics could be performed but are also too expensive. Guidelines suggest simpler models using a 5th order Airy wave model together with Morisson's equations (Sarpkaya 1986). This semi-empirical formula may be integrated on the jacket structure as a boundary condition. Using these hypothesis, a mechanical problem may be formulated and time series of stress at the hot spot may be computed.

2.2 *Mechanical formulation*

This subsection presents a general formulation of the quasi-static mechanical problem. The structure that is modelled may be the whole jacket structure or a part of it.

2.2.1 *Continuous problem*

First, we need to introduce the formulation and numerical solving of the continuous problem to define the discretization error. Let $\mathbb{R}^d$ represent the physical space and Ω the subspace of $\mathbb{R}^d$ occupied by the structure (with d comprised between 1 and 3). This structure is subject to a body force f on Ω, a traction force F on its boundary $\partial_F\Omega$ and a dispacement field $\underline{u}_d$ on $\partial_u\Omega$. Let $\partial_u\Omega \cup \partial_F\Omega = \varnothing$ and $\partial_u\Omega \neq \varnothing$. The structure is assumed to undergo small perturbations and the unknown displacement field is denoted u. The symmetric part of its gradient is the deformation $\underline{\underline{\epsilon}}(\underline{u})$. The material is considered to be linear elastic characterized by Hooke's elasticity tensor $\mathbb{H}$. Let $\underline{\underline{\sigma}}$ be the Cauchy stress tensor such that:

$$\underline{\underline{\sigma}} = \mathbb{H} : \underline{\underline{\epsilon}} \tag{1}$$

The mechanical problem may be written defining two affine subspaces, respectively kinematically and statically admissible:

$$\mathrm{KA} = \left\{ \underline{u} \in \left(\mathrm{H}^1(\Omega)\right)^d,\ \underline{u} = \underline{u}_d \text{ on } \partial_u\Omega \right\} \tag{2}$$

and

$$SA = \left\{ \underline{\underline{\tau}} \in \left(\mathrm{L}^2(\Omega)\right)^{d\times d}_{\text{sym}};\ \forall \underline{v} \in \mathrm{KA}^0,\right.$$

$$\left. \int_\Omega \underline{\underline{\tau}} : \underline{\underline{\epsilon}}(\underline{v})\, d\Omega = \int_\Omega \underline{f} \cdot \underline{v} d\Omega + \int_{\partial_F\Omega} \underline{F} \cdot \underline{v} dS \right\} \tag{3}$$

Where KA^0 is defined with equation 2 for $\underline{u}_d = \underline{0}$.

The error in constitutive relation is defined as a positive form:

$$e_{CR_\Omega}\left(\underline{u}, \underline{\underline{\sigma}}\right) = \| \underline{\underline{\sigma}} - \mathbb{H} : \underline{\underline{\epsilon}}(\underline{u}) \|_{\mathbb{H}^{-1},\Omega} \tag{4}$$

where $\|\underline{\underline{x}}\|_{\mathbb{H}^{-1},\Omega} = \sqrt{\int_\Omega \left(\underline{\underline{x}} : \mathbb{H}^{-1} : \underline{\underline{x}}\right) d\Omega}$

Finally, the mechanical problem to solve reads:

Find a displacement field $\underline{u}_{ex}$ and a stress field $\underline{\underline{\sigma}}_{ex}$ such that:

$$\textit{On } \Omega, \begin{cases} \underline{\underline{\epsilon}}(\underline{u}) = \frac{1}{2}\left(\underline{\underline{\text{grad}}}(\underline{u}) + \underline{\underline{\text{grad}}}(\underline{u})^T\right) \\ \underline{\text{div}}(\underline{\underline{\sigma}}) + \underline{f} = \underline{0} \\ \underline{\underline{\sigma}} = \mathbb{H} : \underline{\underline{\epsilon}}(\underline{u}) \end{cases} \tag{5}$$

$$\textit{On } \partial_u\Omega, \underline{u} = \underline{u}_d$$

$$\textit{On } \partial_F\Omega, \underline{\underline{\sigma}} \cdot \underline{n} = \underline{F}$$

An equivalent formulation of the mechanical problem may be written:

Find a couple $\left(\underline{u}_{ex}, \underline{\underline{\sigma}}_{ex}\right) \in KA \times SA$*, such that* $e_{CR_\Omega}\left(\underline{u}_{ex}, \underline{\underline{\sigma}}_{ex}\right) = 0$

The solution to this problem $\left(\underline{u}_{ex}, \underline{\underline{\sigma}}_{ex}\right)$ exist and is unique. In most cases, this solution cannot be found analytically and the problem is usually discretized.

2.2.2 *Discrete Problem*

Now let us discretize Ω into a tessellation Ω_H of triangles. The finite element method seeks a solution to the mechanical problem in a finite subspace $KA_H \subset KA$, where :

$$KA_H = \left\{\underline{u} \in \left(\mathrm{H}^1(\Omega)\right)^d,\ \underline{u} = \underline{u}_d \text{ on } \partial_u\Omega_H\right\} \tag{6}$$

In practice, this subspace is generated by the *a priori* choice of a function basis of dimension m: $[\phi_i]_{i\in[\![1,m]\!]}$.

The discrete problem (also called forward problem) reads:

Find a couple $\left(\underline{u}_H, \underline{\underline{\sigma}}_H\right)$ *such that:*

$$\underline{u}_H \in KA_H$$

$$\underline{\underline{\sigma}}_H = \mathbb{H} : \underline{\underline{\epsilon}}(\underline{u}_H)$$

$$\forall \underline{v}_H \in KA_H^0,$$

$$\int_{\Omega_H} \underline{\underline{\sigma}}_H : \underline{\underline{\epsilon}}(\underline{v}_H)\, d\Omega = \int_{\Omega_H} \underline{f} \cdot \underline{v}_H d\Omega + \int_{\partial_F\Omega_H} \underline{F} \cdot \underline{v}_H dS \tag{7}$$

The solution of this discrete problem exists and is unique. However, the discrete solution $\underline{u}_H$ usually does not coincide with the continuous exact solution $\underline{u}_{ex}$.

2.2.3 *Computation of error bounds*

Generalities Because the displacement field $\underline{u}_H \neq \underline{u}_{ex}$, the finite element method introduces the discretization error $e_{discr} = \|\underline{u}_H - \underline{u}_{ex}\|_{\mathbb{H},\Omega}$. When the convergence rate of FEM is known *a priori*, an estimate of this error may be computed. However, it is usually impractical because some problem dependent constants are not computable. *A posteriori* error estimators also exist. They rely on a post-process of the finite element solution to derive an estimation of the discretization error (Ainsworth & Oden 1997). This error estimation is easily implemented and computationnally cheap and may be available on industrial codes. This smoothing technique engenders an estimation of error bounds, meaning that e_{discr} may be greater than the estimation (Zienkiewicz & Zhu 1987).

The principle is to seek for an optimized stress field $\underline{\underline{\sigma}}_{opt}$ by smoothing the finite element stress field $\underline{\underline{\sigma}}_H$. To do so, the optimized stress field is decomposed in the same basis $[\phi_i]_{i\in[\![1,m]\!]}$ as for the displacement $\underline{u}_H$. For each node j, the coefficients $\left[\sigma^j_{opt,i}\right]_{i\in[\![1,m]\!]}$ are calculated by averaging the stress field on adjacent elements. An estimator of the discretization error is then obtained using:

$$e_{discr} = \left\|\underline{\underline{\sigma}}_H - \underline{\underline{\sigma}}_{ex}\right\|_{\mathbb{H}^{-1},\Omega} \approx \left\|\underline{\underline{\sigma}}_H - \underline{\underline{\sigma}}_{opt}\right\|_{\mathbb{H}^{-1},\Omega} \tag{8}$$

Other techniques provide strict upper bounds of e_{discr} (see (Ladevèze & Pelle 2004)). They rely on the construction of a statically admissible stress field, which can be an expensive task in terms of computational costs.

Bounds on the quantity of interest As the discretization error e_{discr} is an energetical measure of the error, it is often impractical. Goal-oriented error that aims at providing bounds on the error on a quantity of interest $q(\underline{u})$ have been developped. In this paper, the quantity of interest is considered to be a linear form of the displacement field, defined by extractors (Becker & Rannacher 1996): $q(\underline{u}) = \tilde{L}(\underline{u})$.

For some non-linear norms, specific method to compute bounds on the quantity of interest exist (Strouboulis, Babuŝka, Datta, Copps, & Gangaraj 2000, Rüter & Stein 2006). Another solution would be to linearize the quantity of interest.

To derive an error estimator on a quantity of interest, an adjoint problem is solved. The subspace of statically admissible fields is defined for this new problem as:

$$\widetilde{SA} = \left\{\underline{\underline{\tau}} \in \left(\mathrm{L}^2(\Omega)\right)^{d\times d}_{\text{sym}};\ \forall \underline{v} \in KA^0,\ \int_\Omega \underline{\underline{\tau}} : \underline{\underline{\epsilon}}(\underline{v})\, d\Omega = \tilde{L}(\underline{v})\right\} \tag{9}$$

Finally, the adjoint problem reads:
Find $\left(\underline{\tilde{u}}_{ex}, \underline{\underline{\tilde{\sigma}}}_{ex}\right) \in KA^0 \times \widetilde{SA}$ such that :

$$e_{CR_\Omega}\left(\underline{\tilde{u}}_{ex}, \underline{\underline{\tilde{\sigma}}}_{ex}\right) = 0 \tag{10}$$

The solution to this problem exists and is unique.

The adjoint problem is usually solved using the finite element method. The mesh does not need to be the same as for the forward problem. However, using the same mesh allows to use the same stiffness matrix factorization for both forward and adjoint problems. In the end, solving the two problems is equivalent to solving a multiple right-hand side linear equation.

Let us denote $\underline{\tilde{u}}_{\tilde{H}}$ the adjoint displacement field obtained by solving the adjoint problem with FEM. The discretization error of the adjoint problem reads:

$$\tilde{e}_{discr} = |||\underline{\tilde{u}}_{ex} - \underline{\tilde{u}}_{\tilde{H}}|||_\Omega \approx \left\|\underline{\underline{\tilde{\sigma}}}_H - \underline{\underline{\tilde{\sigma}}}_{opt}\right\|_{\mathbb{H}^{-1},\Omega} \tag{11}$$

Bounds on the quantity of interest $q\left(\underline{u}_{ex}\right)$ can be computed (Ladevèze 2006, Ladevèze 2008) :

$$\left|q\left(\underline{u}_{ex}\right) - q\left(\underline{u}_H\right)\right| \leqslant e_{discr}\tilde{e}_{discr} \tag{12}$$

If the quantity of interest was the stress σ_{11} for example, q would represent the displacement to stress relation together with the extractor of σ_{11} from the tensor $\underline{\underline{\sigma}}$.

Using (12), an interval in which $q\left(\underline{u}_{ex}\right)$ should lie may be defined:

$$q\left(\underline{u}_H\right) - e_{discr}\tilde{e}_{discr} \leqslant q\left(\underline{u}_{ex}\right) \leqslant q\left(\underline{u}_H\right) + e_{discr}\tilde{e}_{discr} \tag{13}$$

3 POST-PROCESSING OF STRESS TIME SERIES AND PROBABILITY OF FAILURE

3.1 *Isolation of stress cycles*

Several methods exist to post-process stress time-series and perform fatigue analysis. Rainflow-counting is the most used (Matsuishi & Endo 1968) but spectrum analysis is also possible (Sherf & Tuestad 1987). Rainflow counting was chosen in this paper as it is usually more precise (Larsen & Irvine 2013).

To isolate stress cycles, the time series is turned at 90^o as shown in Figure 1.

First, turning points are identified within the stress time series. This procedure identifies local maxima and minima of stress over time. The name rainflow counting is an analogy to water flowing down a roof. At each valley of the stress time series (and respectively peak) a droplet is deposed and the water flows down the slope until either:

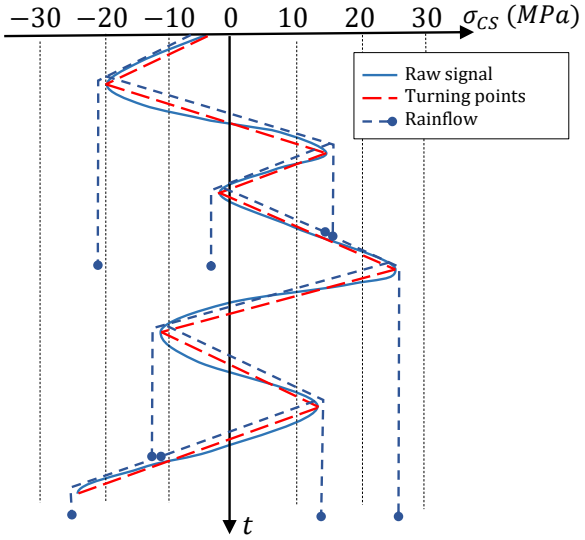

Figure 1: Conversion of signal into turning points and rainflow counting

- It falls from a peak (or respectively a valley) of the signal and either reaches a smaller valley (or respectively a higher peak) than the one from where it started or it reaches another slope
- It is reached by water falling from another valley (or respectively peak)
- It falls beyond every peak

Half cycles can then be identified as the stress difference between the starting valley and the stress at which the droplet stops.

3.2 *Construction of signals bounding damage*

At each timestamp t_k ($k \in [\![1, n_{ts}]\!]$) of the time series, a finite element solution of stress at the hot spot is obtained together with bounds within which the exact solution of the mechanical model lies using (13). It is significantly different from state of the art fatigue analysis for which only a value of stress is known and not an interval in which it lies. Propagating bounds on stress to the damage is not a trivial task. It requires to build two signals passing within every interval delimitated by bounds:

- one maximizing damage thus presenting maximum oscillation
- one minimizing damage and thus presenting minimal oscillations.

To build the signal minimizing damage, it is proposed to use the signal passing for each time stamps t_k at the point within the interval which is the closest to the one selected for t_{k-1}. For t_0, this point is chosen as the closest boundary to the first interval (at $t > t_0$) guaranteed to be above or below the interval at t_0. The sequence of turning points that is then derived is shown in Figure 2. If the value selected at t_{k-1} lies in the interval at t_k, then the signal remains constant.

Otherwise, it will pass by one of the two bounds at t_k. While no formal proof is given, it has been observed to minimize damage as it minimizes oscillation while passing in every interval.

To build the signal maximizing damage, it is proposed to use the signal passing in each interval at the point furthest from signals mean over the whole time frame. This signal is not the one maximizing damage, as a signal with increased damage would oscilate between lower and upper boundaries at succesive time stamps. However, such a signal would be unrealistic as the position of the exact solution within bounds should not change radically over time.

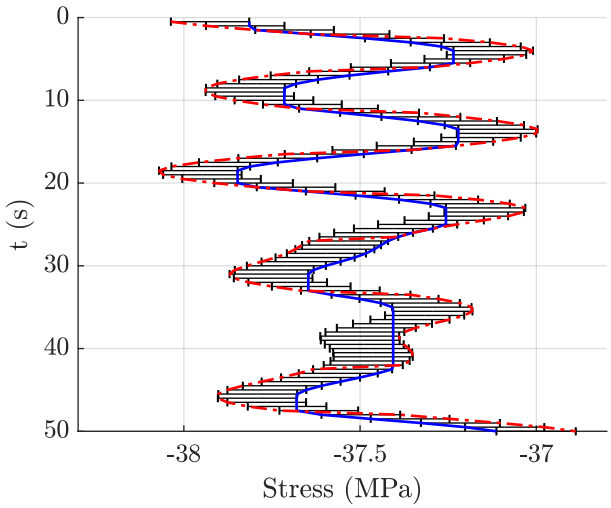

Figure 2: Construction of extreme signals (maximal damage in red dotted line - minimal damage in blue plain line - error bound for each sample in black)

4 PROPAGATION OF BOUNDS ON FATIGUE LIFE

All the cycles stress ranges $\Delta\sigma_i$ ($i \in [1, n_{ts}]$) may then be gathered and converted to maximum number of cycle before failure $sn\left(\Delta\sigma_i\right)$ using SN curves (see Figure 4). The Palmgren-Miner rule may then be used to define the survival of the structure within the deployment time t_{dep} using timeseries of duration $t_{n_{ts}}$ (Palmgren 1959, Miner et al. 1945):

$$g\left(\mathrm{sn}\right) = 1 - \sum_{j=1}^{n_{ss}} \left(\frac{t_{dep}\mathbf{P}\left[H_s(j), T_p(j), \theta_0(j)\right]}{t_{n_{ts}}} D_j \right) \tag{14}$$

Where $\mathbf{P}\left[H_s(j), T_p(j), \theta_0(j)\right]$ is the probability of occurence of each seastate and D_j is the total damage in sea state j and reads:

$$D_j = \sum_{i=1}^{n_{tp}} \frac{1}{\mathrm{sn}\left(\Delta\sigma_i\right)} \tag{15}$$

The function g is positive if the total damage is smaller than one and the structure shall survivre. Otherwise, if g is negative then the structure should fail. In reality, SN-curves are probabilistic and sn should be modelled as a random variable SN. In log-log scale, this random variable is distributed as a Gaussian with bilinear mean and 0.2 standard deviation as prescribed by (Det Norske Veritas 2010). Figure 4 shows random samples of stress and number of cycle before failure together with mean and 97.7% chance of survival curves.

In this paper, a deterministic approach is used with a single sea state (because of available resource). The 97.7% chance of survival SN curve is used in order to obtain a deterministic damage. However, as the use of random SN curve is a post-process of the FEM analysis, propagating bounds to the probability of failure would be straightforward if multiple sea states were used.

5 NUMERICAL ASSESSMENT

The proposed method was applied on a numerical example in order to illustrate the performance of the approach. It was chosen to study an electical substation developped by Chantiers de l'Atlantique for offshore wind farms (see Figure 5). The part of the structure that was studied is the connection piece between the jacket structure and the pile sleeve: the shear plate (see Figure 6). Due to its position, the wind dynamical loads do not affect the shear plate and therefore its mechanical response can be considered quasi-static

The weld toe between the shear plate and the pile sleeve was chosen as the hot spot where fatigue analysis was conducted. Because of available resource, it was proposed to use sub-modelling. As depicted in Figure 3, the whole substation structure (including the shear plate) was first simulated in order to derive resulting loads at the boundary of the shear plate. These loads are then used as boundary conditions to a second mechanical problem aiming at computing hot spot stress on the shear plate. For both simulations, the material was considered as isotropic, linear and elastic with steel standard Young modulus and Poisson ratio (respectively $E = 210GPa, \nu = 0.3$). The following two subsections present the complete problem on the whole structure and the problem on the shear plate.

5.1 *Jacket structure mechanical model*

The jacket structure was modeled as a 3D structure of beam and shell elements. The quasi-statical response was run in a single sea state ($H_s = 2m, T_p = 10$) because of available resource. The wave model was chosen as a superimposition of 50 Airy waves and the load model was chosen as Morison as prescribed in (Det Norske Veritas 1996). The time discretization was chosen as 20 time stamps per peak wave which

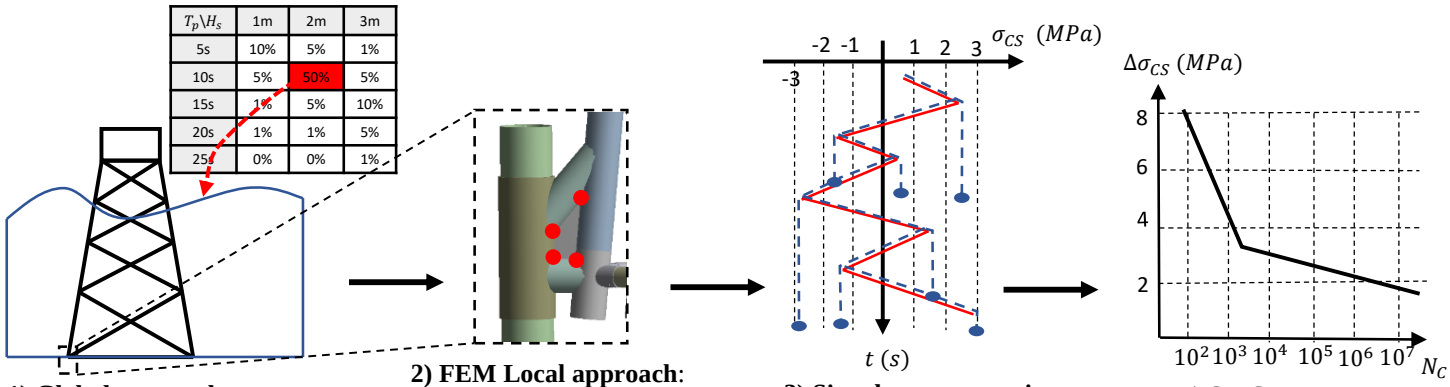

1) Global approach:
Output: 3h timeseries of stress close at 4 nodes delimitating the shear plate

2) FEM Local approach:
Output: 3h timeseries of stress close at the weld toe suspected to fail together with bounds on the exact value

3) Signal post-processing using Rainflow counting:
Output: Stress cycles for the FEM signal and bounds

4) SN Curve
Output: Damage

Figure 3: General workflow

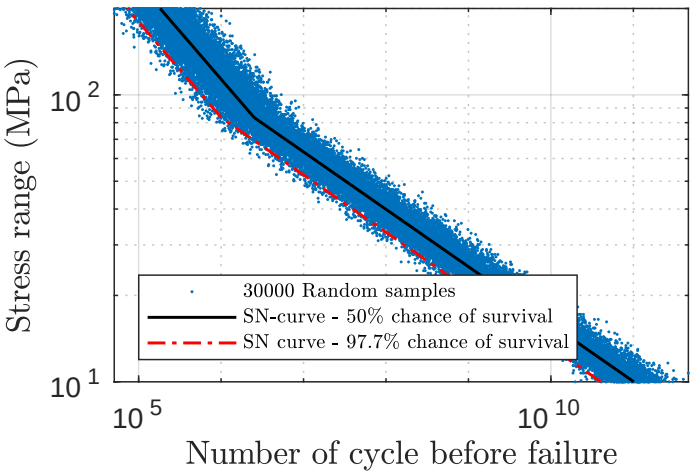

Figure 4: Random samples of stress and number of cycle to failure together with mean and 97.7% chance of survival curves

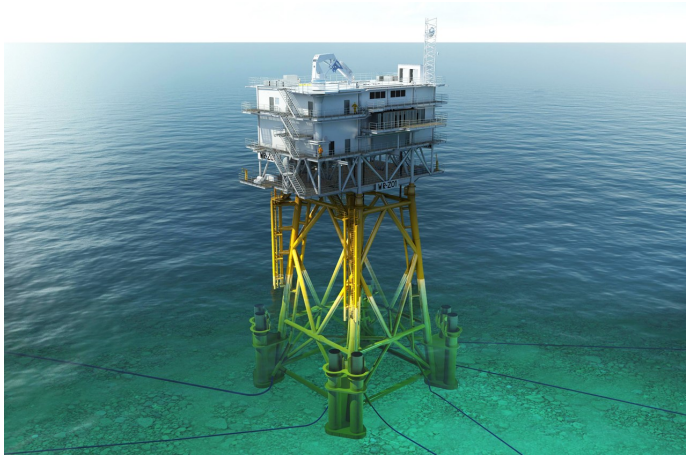

Figure 5: Westermost Rough (UK) electrical substation (ⓒChantiers de l'Atlantique)

corresponds to 0.5s intervals. Tensile stress time series was derived in the 4 tubulars at the 4 nodes delimitating the shear plate as shown in Figure 7 using ANSYS®.

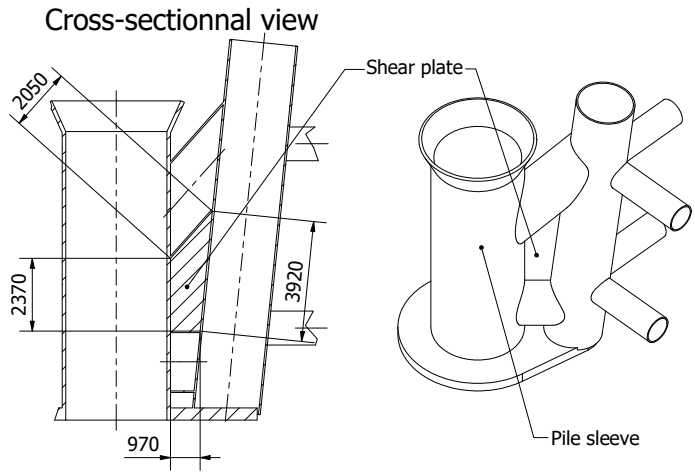

Figure 6: Shear plate geometry

5.2 *Shear plate mechanical model*

The shear plate was modeled in 2D plane stress as its thickness ($e = 50mm$) is negligible compared to the plate main dimensions depicted in Figure 6. Force was imposed as a boundary condition on the 4 edges delimitated by tubulars (A, B, C, D) and constituting $\partial_F\Omega$ in 3. These boundary conditions were modelled as a linear interpolation of tensile stress calculated on the global structure. To block every motion of rigid body, translations and out of plane rotations were blocked for node 2 (resulting in a pivoting link) and node 3 was blocked in vertical translation (punctiform joint) as depicted in Figure 7.

The method to calculate local stress at the weld toe follows the method prescribed by (Det Norske Veritas 2010). The resolution of the mechanical problem by the finite element method results in the calculation of the stress tensor at $N_{0.5}$, the point distant of $0.5e$ from the weld toe. In the weld toe local basis $(\vec{e}_{\parallel}, \vec{e}_{\perp})$, the stress tensor reads :

$$\underline{\underline{\sigma}}_{N_{0.5}} = \begin{pmatrix} \sigma_{\parallel} & \tau_{\parallel} \\ \tau_{\parallel} & \sigma_{\perp} \end{pmatrix} \quad (16)$$

The quantity of interest for further fatigue analysis is calculated as the maximal principal stress at node

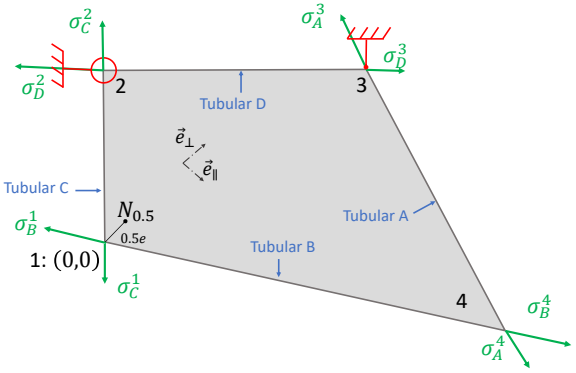

Figure 7: Shear plate mechanical problem and hot spot $N_{0.5}$ location (e: plate thickness)

$N_{0.5}$ with an extrapolation factor of 1.12 to account for the weld toe concentration:

$$\sigma_1 = 1.12 \max \left\{ \begin{array}{c} \sqrt{\sigma_\perp^2 + 0.81\tau_\parallel} \\ a \left| \frac{\sigma_\perp + \sigma_\parallel}{2} + \frac{1}{2}\sqrt{\left(\sigma_\perp - \sigma_\parallel\right)^2 + 4\tau_\parallel^2} \right| \\ a \left| \frac{\sigma_\perp + \sigma_\parallel}{2} - \frac{1}{2}\sqrt{\left(\sigma_\perp - \sigma_\parallel\right)^2 + 4\tau_\parallel^2} \right| \end{array} \right. \tag{17}$$

With $a = 0.90$ for this detail manually welded from both side with full penetration.

The quantity σ_1 being non linear against the differents stress components, obtaining error bound indicators is possible but more difficult. For this contribution and as the shear plate mainly overcomes shear stress, it was considered that $\left(\sigma_\parallel, \sigma_\perp\right) << \tau_\parallel$. The quantity of interest finally reads:

$$\sigma_1 = 1.008\tau_\parallel \tag{18}$$

The simulations were run using a homemade FEM code and post-processed in Matlab. The WAFO toolbox was used to isolate stress cycles (Brodtkorb, Johannesson, Lindgren, Rychlik, Rydén, Sjö, et al. 2000). The SN curve for this structural detail was chosen as the D-curve in seawater with cathodic protection from (Det Norske Veritas 2010). It is plotted in Figure 4.

5.3 *Results*

The signal of the quasi-static FEM solution together with error bound were computed for the shear plate mechanical problem on the 3h time frame. Two meshes were tested. Both meshes are non uniform as the density is higher near the hot spot (see Figure 8).

The coarse mesh uses the mesh size prescribed by (Det Norske Veritas 2010) at the hot spot (i.e. 50mm). The fine mesh is much smaller at the hot spot: 3.3mm. Figure 9 shows the two signals of error indicators.

There is no intersection between the error indicators computed with the fine mesh and the ones with

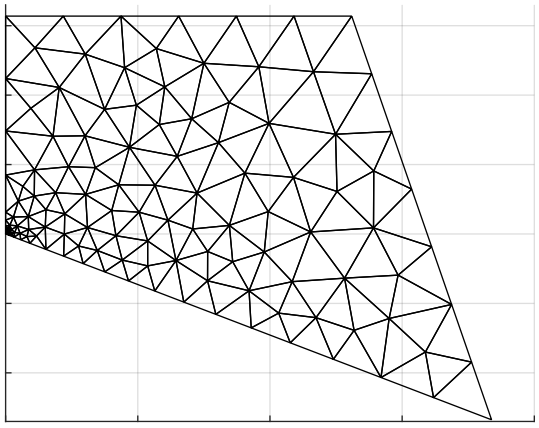

Figure 8: Fine mesh

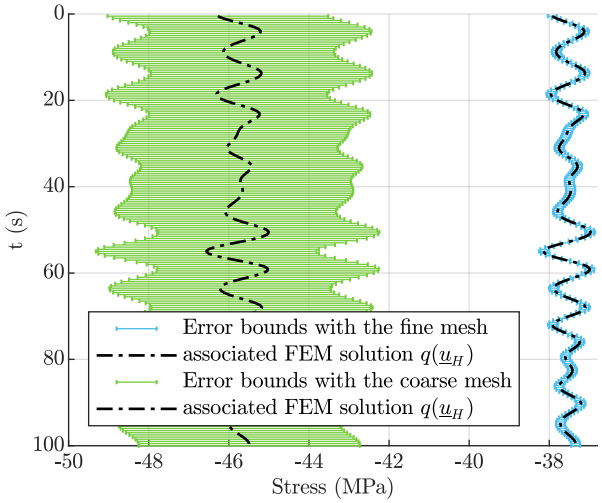

Figure 9: Error bounds signals for two different meshes

the coarse mesh. For guaranteed bounds, the exact solution would be at the intersection of bounds calculated on different meshes. Therefore, the exact solution of the mechanical problem is not guaranteed to lie within error indicators in this paper. This plot shows that pure shear stress evaluated with FEM is not converged with the coarse mesh for this mechanical problem (variation of 19% with mesh size 3.3mm). Table 1 shows error bounds estimation on the total damage D together with the damage computed for the FEM solution for the two meshes.

Mesh size	Lower bound on D	FEM D	Upper bound on D
50 mm	0	1.01×10^{-13}	1.23×10^{-10}
3.3 mm	1.22×10^{-14}	2.51×10^{-14}	4.88×10^{-14}

Table 1: Total damage of the FEM solution and error bound indicators

First, one will notice that the *damage* is in the range of 10^{-14} which is very small. In fact, it might be seen on Figure 9 that the stress cycles are in the range of 1MPa. Such cycles have a very high number of cycles before failure according to Figure 4.

The reason why cycles have a low stress range

might be that the sea state that was chosen is too calm. A more energetical sea state might produce higher stress ranges and therefore more damage to the shear plate. A second reason why the stress ranges are low might be that maximal principal stress at the hot spot is not always in pure shear. A better assessment might be performed by considering $\sigma_{\parallel}$ and $\sigma_{\perp}$ together with $\tau_{\parallel}$. Finally, only tensile stress is imposed as a boundary condition, bending moments might have to be applied in order to fully capture loads causing fatigue.

It may be seen that calculated on the fine mesh, error indicators on the damage are comprised within the ones calculated on the coarse mesh. This was not the case for σ_1. It may suggest that the exact solution to the damage might lie in the computed interval.

It may be seen that there is a factor 4 between the coarse and the fine mesh on the damage calculated with the FEM solution. While the damage is not converged on the coarse mesh, the upper bound being in the range 10^{-10} might suggest that this sea state does not produce fatigue and that the coarse mesh is sufficient for fatigue analysis of this sea states (as prescribed by (Det Norske Veritas 2010). In a more complete analysis including multiple sea states, the contribution of each sea state to the total damage and to the error bounds on the total damage might allow to select the sea state to be calculated on the fine mesh, thus reducing the error on total damage.

6 CONCLUSION

In this paper, an innovative method to propagate discretization error indicators due to FEM on damage was presented. These error bounds on stress are computed by post-processing the finite element solution. The exact solution of the mechanical problem is not guaranteed to lie within error indicators. However, it is computationnaly cheap and appropriate to make sure that the mesh selected to perform fatigue analysis using FEM is adequate. In fact, these bounds may guide remeshing if the error on the value of the total damage is too high.

Future work will first focus on using multiple sea states in order to propagate error bounds to the probability of failure in fatigue while using goal oriented remeshing in order to reduce the uncertainty on the exact value of the probability of failure. Then, a more complete analysis will be computed using the maximal principal stress instead of only using the pure shear component. A 3D model of both the shear plate, weld toes and tubulars may then be used in order to further underline the benefits of goal oriented remeshing strategies on fatigue analysis. Finally, the use of guaranteed bounds on the quantity of interest will be considered in order to provide guaranteed bounds on the damage and the probability of failure instead of bound indicators as used in this paper.

ACKNOWLEDGEMENT

This work was carried out within the project MUSCAS (MUlti-SCAle Stochastic computation for MRE) granted by WEAMEC, WEst Atlantic Marine Energy Community with the support of Région Pays de la Loire and in partnership with Chantiers de l'Atlantique.

REFERENCES

Ainsworth, M. & J. T. Oden (1997). A posteriori error estimation in finite element analysis. *Computer methods in applied mechanics and engineering 142*(1-2), 1–88.

Becker, R. & R. Rannacher (1996). A feed-back approach to error control in finite element methods: Basic analysis and examples. *Journal of Numerical Mathematics 4*, 237–264.

Brodtkorb, P. A., P. Johannesson, G. Lindgren, I. Rychlik, J. Rydén, E. Sjö, et al. (2000). WAFO - a Matlab toolbox for analysis of random waves and loads. In *Proc. 10th Int. Offshore and Polar Eng. Conf., ISOPE, Seattle, USA*, Volume 3, pp. 343–350.

Ciarlet, P. (1978). *The Finite Element Method for Elliptic Problems*. Studies in Mathematics and its Applications. Elsevier Science.

Det Norske Veritas (1996). Guideline for offshore structural reliability analysis: application to jacket platforms. Technical report, Technical report, DNV, Oslo.

Det Norske Veritas (2010). Fatigue design of offshore steel structures. *DNV Recommended Practice DNV-RP-C203*.

Ladevèze, P. (2006). Upper error bounds on calculated outputs of interest for linear and nonlinear structural problems. *Comptes Rendus Académie des Sciences - Mécanique, Paris 334*(7), 399–407.

Ladevèze, P. (2008). Strict upper error bounds on computed outputs of interest in computational structural mechanics. *Computational Mechanics 42*(2), 271–286.

Ladevèze, P. & J. P. Pelle (2004). *Mastering Calculations in Linear and Nonlinear Mechanics*. New York: Springer.

Larsen, C. E. & T. Irvine (2013). A review of spectral methods for variable amplitude fatigue prediction and new results.

Matsuishi, M. & T. Endo (1968). Fatigue of metals subjected to varying stress. *Japan Society of Mechanical Engineers, Fukuoka, Japan 68*(2), 37–40.

Miner, M. et al. (1945). Cumulative fatigue damage. *Journal of applied mechanics 12*(3), A159–A164.

Palmgren, A. (1959). Ball and roller bearing engineering. *Philadelphia: SKF Industries Inc., 1959*.

Rüter, M. & E. Stein (2006). Goal-oriented a posteriori error estimates in linear elastic fracture mechanics. *Computer methods in applied mechanics and engineering 195*(4-6), 251–278.

Sarpkaya, T. (1986). Force on a circular cylinder in viscous oscillatory flow at low keulegancarpenter numbers. *Journal of Fluid Mechanics 165*, 61–71.

Sherf, I. & T. Tuestad (1987). Fatigue design of the oseberg jacket structure. In *Proc. OMAE*.

Strouboulis, T., I. Babuŝka, D. Datta, K. Copps, & S. Gangaraj (2000). A posteriori estimation and adaptive control of the error in the quantity of interest. part i: A posteriori estimation of the error in the von mises stress and the stress intensity factor. *Computer Methods in Applied Mechanics and Engineering 181*(1-3), 261–294.

Zienkiewicz, O. C. & J. Z. Zhu (1987). A simple error estimator and adaptive procedure for practical engineerng analysis. *International journal for numerical methods in engineering 24*(2), 337–357.